

Electrochemistry of Metal Phthalocyanines in Organic Solvents at Variable Pressure

Bazhang Yu,[†] A. B. P. Lever,[‡] and Thomas W. Swaddle^{*†}*Department of Chemistry, University of Calgary, Calgary, Alberta, Canada T2N 1N4, and Department of Chemistry, York University, Toronto, Ontario, Canada M3J 1P3*

Received February 26, 2004

High-pressure electrochemical investigations of representative metallophthalocyanines in solution are reported. The selected systems were ZnPc, CoPc, FePc, and CoTNPc (Pc = phthalocyanine, TNPc = tetraeopentoxypthalocyanine) in several donor solvents and (for CoTNPc) dichlorobenzene, with [Bu₄N][ClO₄] as supporting electrolyte and a conventional Pt electrode referred to Ag⁺(CH₃CN)/Ag. Electrode reaction volumes ΔV_{cell} for CoTNPc and ZnPc show that consecutive ring reductions result in progressive increases in electrostriction of solvent in accordance with Drude–Nernst theory. Reductions of the metal center in CoTNPc and CoPc, however, result in much less negative values of ΔV_{cell} than would be expected by analogy with ring reductions of the same charge type. This is attributable to loss of axial ligands following the insertion of antibonding 3d_{z²} electrons on going from Co^{III} to low-spin Co^{II} and then Co^I. In the same vein, rate constants for reduction of Co^{III} centers to Co^{II} were an order of magnitude slower than those for other metal center or phthalocyanine ring reductions because of Franck–Condon restrictions. The volumes of activation $\Delta V_{\text{el}}^{\ddagger}$ were invariably positive for all the electrode reactions and in most cases were roughly equal to the volumes of activation for reactant diffusion $\Delta V_{\text{diff}}^{\ddagger}$, indicating predominant rate control by solvent dynamics rather than by activation in the manner of transition-state theory for which negative $\Delta V_{\text{el}}^{\ddagger}$ values are expected. For CoTNPc and CoPc in donor solvents, the ΔV_{cell} and $\Delta V_{\text{el}}^{\ddagger}$ data are consistent with the assignments of the successive reduction steps made for CoTNPc in DMF by Nevin et al. (*Inorg. Chem.* **1987**, *26*, 570).

Introduction

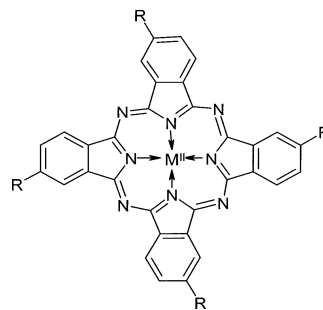
We report here the first study of the effects of pressure on the potentials and kinetics of electrode reactions of representative metallophthalocyanines (Chart 1) in organic solvents.

The dependence of the potential E_{cell} of an electrode half-reaction (conventionally written as a reduction) on pressure P relative to a particular reference half-cell can be expressed as a cell reaction volume, ΔV_{cell} :

$$\Delta V_{\text{cell}} = -nF(\partial E_{\text{cell}}/\partial P)_T \quad (1)$$

Here n is the number of electrons transferred and F is 96 485 A s mol⁻¹. Since the change in the charge number z of the reactant necessarily involves solvational changes, it is useful to regard ΔV_{cell} as being the sum of three parts: an

Chart 1. Metal Phthalocyanines Investigated in This Work (R = H with M = Fe, Co, Zn; R = -OCH₂C(CH₃)₃ with M = Co)



intrinsic part ΔV_{int} , comprising any change in the effective volume of the reactant (due, e.g., to bond length changes or ligand loss); the contribution ΔV_{ref} of the reference electrode; the volume effect ΔV_{solv} accompanying the change in solvent electrostriction around the reactant.

$$\Delta V_{\text{cell}} = \Delta V_{\text{int}} + \Delta V_{\text{ref}} + \Delta V_{\text{solv}} \quad (2)$$

* Author to whom correspondence should be addressed. E-mail: swaddle@ucalgary.ca. Tel.: (403) 220-5358. Fax: (403) 284-1372.

[†] University of Calgary.

[‡] York University.

We have shown elsewhere⁴ that ΔV_{ref} can be taken as constant (i.e., that the pressure dependence of the liquid junction potential is negligible) for a particular reference electrode with organic solvents such as are considered in this study. According to the Drude–Nernst theory,^{1–4} for a reactant molecule or ion of effective radius r in a solvent of static dielectric constant ϵ , the last term in eq 2 is given by

$$\Delta V_{\text{soln}} = -[N_{\text{A}} e^2 / 8\pi\epsilon_0 r] \Phi \Delta(z^2) \quad (3)$$

where $\Phi = (1/\epsilon)(\partial \ln \epsilon / \partial P)_T$, if r is independent of the change $\Delta(z^2)$ in the charge number z resulting from electron transfer. We have recently discussed the origins of eqs 2 and 3 and have shown that, for the decamethylferrocene(+/0) couple in organic solvents with constant ΔV_{int} and ΔV_{ref} , ΔV_{cell} is indeed a linear function of Φ .⁴ Previously, Tregloan and co-workers² had studied a series of complexes $[\text{Fe}(\text{CN})_x \text{L}_{(3-x/2)}]^{(3-x)/(2-x)}$ (bidentate $\text{L} = \text{phen}$ or bpy , $x = 0–6$) for which r (and hence ΔV_{int}) does not change significantly following electron transfer and found a linear dependence of ΔV_{cell} on $\Delta(z^2)$ in aqueous KNO_3 with constant ΔV_{ref} . One objective of the present study was to examine the dependence of ΔV_{cell} on $\Delta(z^2)$ for successive electron transfers to a particular molecule in nonaqueous solvents, and for this purpose some phthalocyanines of Zn, Fe, and Co were selected (Chart 1).

Conversely, it was anticipated that new insights would be gained into the electrochemistry of metal phthalocyanines, a class of compounds of intrinsic scientific interest and with numerous applications—for example as pigments, chemical sensors, laser dyes, and catalysts for fuel cells and pollution control and in liquid crystal color displays and information storage technology.⁵ Zinc(II) phthalocyanine was chosen as a reference system because only the ring system undergoes oxidation or reduction, whereas electron transfer to Fe and Co phthalocyanines can involve either the ring or the central metal atom.

An attempt has also been made to obtain comparative kinetic data on the electrode reactions of the same metal phthalocyanines. The standard (i.e., zero-overpotential) rate constant k_{el} for the electrode reaction of a couple in solution is notoriously difficult to measure absolutely, as it is susceptible to changes in the nature of the electrode surface, to double-layer effects, and (particularly in organic solvents) to artifacts due to the uncompensated resistance R_{u} of the cell;⁶ for example, reported k_{el} values for the ferrocene(+/0) couple in acetonitrile at a Pt electrode at 25 °C range from 0.02 to 220 cm s^{-1} , although most cluster around 1–4 cm s^{-1} .⁷ One can, however, make useful comparisons

between k_{el} values obtained under closely similar conditions. By the same token, the volume of activation $\Delta V_{\text{el}}^\ddagger$ ($= -RT(\partial \ln k_{\text{el}} / \partial P)_T$) for an electrode reaction can be satisfactorily reproducible even when k_{el} shows disquieting scatter between replicate experiments, since $\Delta V_{\text{el}}^\ddagger$ is obtained from relative values of k_{el} within a given run with the same electrodes and, moreover, moderate pressure does not affect the nature of an electrode. If, as is usually the case,^{3,4} $\Delta V_{\text{el}}^\ddagger$ is not dependent on pressure within the experimental uncertainty, $\ln k_{\text{el}}$ becomes a linear function of the applied pressure P :

$$\ln k_{\text{el}} = \ln k_{\text{el}}^0 - P\Delta V_{\text{el}}^\ddagger / RT \quad (4)$$

Here k_{el}^0 is the standard electrochemical rate constant at zero applied (i.e., atmospheric) pressure. The electrochemical experiments also yield values of the mean diffusion coefficient D of the electroactive species, the pressure dependence of which can be similarly represented by a volume of activation for diffusion $\Delta V_{\text{diff}}^\ddagger$ ($= -RT(\partial \ln D / \partial P)_T$) which, for organic solvents, is also effectively independent of pressure:

$$\ln D = \ln D^0 - P\Delta V_{\text{diff}}^\ddagger / RT \quad (5)$$

As discussed below, comparison of $\Delta V_{\text{diff}}^\ddagger$ with $\Delta V_{\text{el}}^\ddagger$ can be uniquely informative regarding the mechanism of the electrode reaction.⁴

Experimental Section

Materials. Zinc phthalocyanine (ZnPc) was prepared from phthalonitrile, zinc chloride, and hydroquinone by the method of Thompson et al.⁸ The product was purified by Soxhlet extraction with water and then acetone for 24 h each. Iron(II) phthalocyanine (FePc, Fluka) and cobalt(II) phthalocyanine (CoPc, Aldrich) were used as received. (2,9,16,23-Tetraneopentoxophthalocyaninato)-cobalt(II) (CoTNPC) was prepared by the method of Leznoff et al.⁹ except that the eluent in the flash column chromatographic purification step was ethyl acetate–hexane (1:5) rather than toluene. The purity of the dark blue crystalline product was established from its NMR and UV–visible spectra in *N,N*-dimethylformamide (DMF).

The solvents used for electrochemistry [DMF, Aldrich, 99.8%; *N,N*-dimethylacetamide (DMA), Baker Analyzed Reagent; dimethyl sulfoxide (DMSO), Aldrich, 99.9%; pyridine (Py), Aldrich, 99+%; *o*-dichlorobenzene (DCB), Pfalz & Bauer, 98%] were dried over molecular sieves and redistilled under reduced pressure. DMA and DCB in particular were always distilled immediately before use. Tetrabutylammonium perchlorate (TBAP; Fluka electrochemical grade, >99%) was used as received.

Electrochemical Measurements. Cyclic voltammetry (CV) and differential-pulse polarography (DPP) (for measurements of E_{cell} and mean diffusion coefficients D for the electrochemically active species) and alternating current voltammetry (ACV) (to determine k_{el}) were performed using an EG&G Princeton Applied Research model 273 potentiostat, a model 5208 two phase lock-in analyzer,

(1) Isaacs, N. S. *Liquid-Phase High-Pressure Chemistry*; Wiley: New York, 1981; Chapter 2.

(2) Sachinidis, J. I.; Shalders, R. D.; Tregloan, P. A. *Inorg. Chem.* **1994**, *33*, 6180.

(3) Swaddle, T. W.; Tregloan, P. A. *Coord. Chem. Rev.* **1999**, *187*, 255.

(4) Matsumoto, M.; Swaddle, T. W. *Inorg. Chem.* **2004**, *43*, 2724.

(5) *Phthalocyanines: Properties and Applications*; Leznoff, C. C., Lever, A. B. P., Eds.; VCH: New York, 1989, 1993, 1996; Vols 1–4.

(6) Weaver, M. J. *Chem. Rev.* **1992**, *92*, 463.

(7) Fawcett, W. R.; Opallo, M. *Angew. Chem., Int. Ed. Engl.* **1994**, *33*, 2131.

(8) Thompson, J. A.; Murata, K.; Miller, D. C.; Stanton, J. L.; Broderick, W. E.; Hoffmann, B. M.; Ibers, J. A. *Inorg. Chem.* **1993**, *32*, 3546.

(9) Leznoff, C. C.; Marcuccio, S. M.; Greenberg, S.; Lever, A. B. P.; Tomer, K. B. *Can. J. Chem.* **1985**, *63*, 623.

and a model 174A polarographic analyzer. In CV, E_{cell} was obtained by taking the average of corresponding anodic and cathodic peak potentials (the separation of CV peaks is to some extent dependent upon the kinetics of the electrode reaction, but the average potential is unaffected). DPP was used to measure D and the volume of activation for diffusion $\Delta V_{\text{diff}}^{\ddagger}$ only in some reactions with poorly defined CV peaks. DPP, performed at a low scan rate (2–10 mV/s), gave better peak resolution for twin peaks or slow reactions than did CV, but because cyclic DPP sweeps were not possible with the available equipment, accumulation of reactive electrochemical products tended to cause degradation of the signal. For this reason, CV was used preferentially for measurements of D and $\Delta V_{\text{diff}}^{\ddagger}$, although the numerical results were essentially identical for CV and DPP.

The electrochemical cell (Figure S1 in the Supporting Information) was similar to that described previously except that the cell body was machined from stainless steel rather than Teflon for improved thermal conductivity and sealing with the O-rings. Both working and counter electrodes were 0.5 mm diameter Pt wires. For all high-pressure measurements, the reference electrode was Ag/(0.01 mol L⁻¹ AgClO₄ + 0.2 mol L⁻¹ TBAP in acetonitrile) ("Ag/Ag⁺"). For purposes of correlation with literature data relative to SCE, however, CV half-wave potentials E_{cell} were first measured at atmospheric pressure and 25.0 °C and referred internally to the ferrocenium/ferrocene (Fc⁺/Fc) couple (about -0.16 V relative to Ag/Ag⁺)^{11,12} for conversion to values E_{SCE} relative to SCE (corrections applied: +0.49 V for DCB as solvent; +0.40 V for DMF; +0.47 V for DMA; +0.50 V for Py and DMSO¹³). The cell was then placed inside the pressure vessel previously described,¹⁰ the temperature of which was controlled to 25.0 ± 0.1 °C for all solvents except DMSO (45.0 ± 0.1 °C to avoid freezing at high pressure¹⁴) with water circulating through an aluminum jacket, and the vessel was pressurized with hexane.

The key to obtaining reproducible ACV data was minimization of interference by O₂. Oxygen reduction occurred at ~-1.0 V vs SCE, near the middle of the potential window studied (usually -1.8 to +1.0 V vs SCE). All solutions for electrochemical measurement purposes were purged with solvent-saturated nitrogen gas within a drybox or drybag for 2 to 3 h. To avoid ingress of atmospheric oxygen, the filled cell was placed in the pressure vessel immediately after purging and the initial hydrostatic pressure of ~5 MPa was quickly applied to the cell. At higher pressures, oxygen interference vanished completely if O₂ removal and sealing of the cell had been successful.

Theoretical and experimental aspects of electrochemistry at variable pressure have been described previously.^{3,4,10,15–18} For ACV measurements on phthalocyanine complexes, the most appropriate frequency range was 25–75 Hz. In the case of a relatively slow reaction such as the oxidation of [Co^{II}(TNPC²⁻)] to [Co^{III}(TNPC²⁻)]⁺,

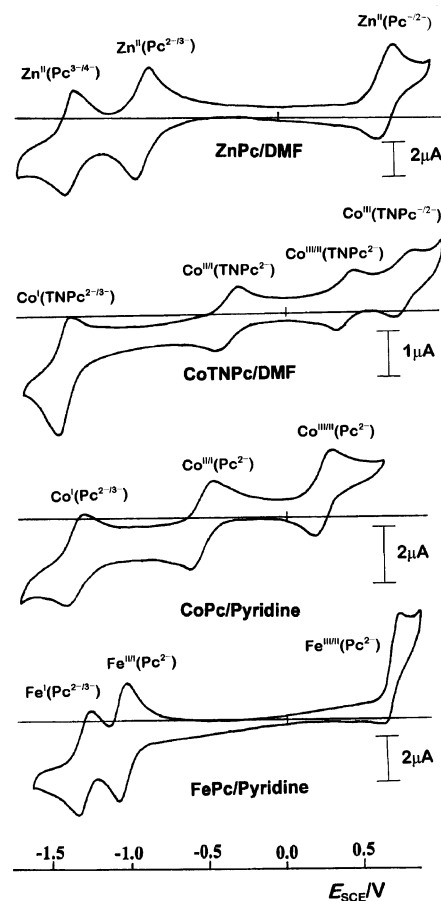


Figure 1. Cyclic voltammograms of ZnPc, CoTNPC, CoPc, and FePc (0.4 mmol L⁻¹) at 25 °C in donor solvents containing 0.2 mol L⁻¹ of TBAP: Pt wire working electrode; scan rate 50 mV s⁻¹. Potentials are displayed relative to SCE.

a lower frequency range (e.g. 15–55 Hz) was necessary to give correctly shaped in-phase and 90°-out-of-phase current peaks, and because the reaction rate became even slower with increasing pressure, the practical upper limit of pressure was ~160 MPa. Calculation of k_{el} from the in-phase and out-of-phase peaks was carried out as described previously,¹⁵ with specific correction for the uncompensated resistance using values of R_u measured at 10 kHz.

Results

As is typical of metal phthalocyanines,⁵ solubility limited the scope of experiments. Of the unsubstituted phthalocyanines considered here, ZnPc was sufficiently soluble (0.2–0.4 mmol L⁻¹) for electrochemistry in Py, DMF, DMSO, and DMA, whereas CoPc and FePc were sufficiently soluble in Py (which evidently coordinates strongly to the Co and Fe centers¹³) but too poorly soluble in DMF, DMSO, and DMA. All were insoluble in acetone. Attention was therefore focused on CoTNPC, in which the bulky neopentoxy groups confer satisfactory solubility in DMF, DMSO, DMA, acetone, and also DCB, although its solubility in Py was inadequate and decomposition occurred in acetone.

Figure 1 shows broad-sweep CVs for ZnPc, CoTNPC, CoPc, and FePc in various solvents, using the high-pressure electrochemical cell at atmospheric pressure. For CoTNPC

- (10) Fu, Y.; Swaddle, T. W. *J. Am. Chem. Soc.* **1997**, *119*, 7137.
 (11) Gagne, R. R.; Koval, C. A.; Lisensky, G. C. *Inorg. Chem.* **1980**, *19*, 2854.
 (12) Gritzner, G.; Kuta, J. *Electrochim. Acta* **1984**, *29*, 869.
 (13) Lever, A. B. P.; Milaeva, E. R.; Speier, G. In *Phthalocyanines: Properties and Applications*; Leznoff, C. C., Lever, A. B. P., Eds.; VCH: New York, 1993; Vol. 3, Chapter 1.
 (14) Fuchs, A. H.; Ghelfenstein, M.; Szwarc, H. *J. Chem. Eng. Data* **1980**, *25*, 206.
 (15) Fu, Y.; Cole, A. S.; Swaddle, T. W. *J. Am. Chem. Soc.* **1999**, *121*, 10410.
 (16) Matsumoto, M.; Lamprecht, D.; North, M. R.; Swaddle, T. W. *Can. J. Chem.* **2001**, *79*, 1864.
 (17) Zhou, J.; Swaddle, T. W. *Can. J. Chem.* **2001**, *79*, 841.
 (18) Swaddle, T. W. In *High-Pressure Chemistry*; van Eldik, R., Klärner, F. G., Eds.; Wiley-VCH: Weinheim, Germany, 2002; pp 161–183.

Table 1. Electrochemical Parameters for ZnPc in Various Solvents^a

solvent	couple	E_{SCE}/V	$\Delta V_{cell}/cm^3 mol^{-1}$	$D/10^{-6} cm^2 s^{-1}$	$\Delta V_{diff}^{\ddagger}/cm^3 mol^{-1}$	$k_{el}/10^{-2} cm s^{-1}$	$\Delta V_{el}^{\ddagger}/cm^3 mol^{-1}$
Py	$[Zn^{II}(Pc^{-2-})]^{+0}$	0.70	-25.9 ± 2.1^b	13.1 ± 0.1	15.8 ± 0.4		
	$[Zn^{II}(Pc^{2-/3-})]^{0/-}$	-0.88	-34.1 ± 0.7	8.4 ± 0.2	11.5 ± 0.4	12.6 ± 0.1	12.4 ± 0.1
	$[Zn^{II}(Pc^{3-/4-})]^{-2-}$	-1.37	-43.8 ± 0.7	8.0 ± 0.1	11.8 ± 0.4	13.5 ± 0.3	13.6 ± 0.5
DMF	$[Zn^{II}(Pc^{-2-})]^{+0}$	0.67	-10.6 ± 0.8	7.1 ± 0.1	10.1 ± 0.5	9.8 ± 0.1	12.6 ± 0.3
	$[Zn^{II}(Pc^{2-/3-})]^{0/-}$	-0.90	-20.8 ± 1.3	7.0 ± 0.1	9.9 ± 1.2	15.5 ± 1.5	12.2 ± 1.8
	$[Zn^{II}(Pc^{3-/4-})]^{-2-}$	-1.38	-30.2 ± 1.3	8.7 ± 0.1	9.7 ± 0.7	10.3 ± 0.9	12.5 ± 1.6
DMSO	$[Zn^{II}(Pc^{-2-})]^{+0}$	0.74	-19.7 ± 0.6^c	4.5 ± 0.1^c	14.1 ± 0.2^c	8.6 ± 0.3^c	17.5 ± 0.7^c
	$[Zn^{II}(Pc^{2-/3-})]^{0/-}$	-0.86	-35.7 ± 0.6^c	6.2 ± 0.1^c	14.8 ± 0.6^c	15.6 ± 0.1^c	15.5 ± 0.2^c
	$[Zn^{II}(Pc^{3-/4-})]^{-2-}$	-1.36	-43.2 ± 0.7^c	7.1 ± 0.1^c	14.7 ± 1.1^c	10.1 ± 0.1^c	15.2 ± 0.1^c
DMA	$[Zn^{II}(Pc^{-2-})]^{+0}$	0.78	-7.3 ± 0.8	2.7 ± 0.1	14.1 ± 0.5^c	4.4 ± 0.1	13.1 ± 0.6

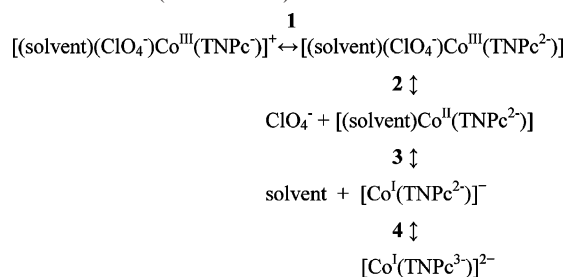
^a At Pt wire; 0.2–0.3 mol L⁻¹ TBAP; [ZnPc] = 0.2–0.4 mmol L⁻¹; 25.0 °C except as noted; reference electrode for ΔV_{cell} is Ag/(0.01 mol L⁻¹ AgClO₄ + 0.2 mol L⁻¹ TBAP in CH₃CN). Formulas given are exclusive of any coordinated solvent or anions. ^b By DPP. ^c 45.0 °C.

Table 2. Electrochemical Parameters for Complexes of Pc and TNPc with Metals of Variable Oxidation States^a

couple	solvent	E_{SCE}/V	$\Delta V_{cell}/cm^3 mol^{-1}$	$D/10^{-6} cm^2 s^{-1}$	$\Delta V_{diff}^{\ddagger}/cm^3 mol^{-1}$	$k_{el}/10^{-2} cm s^{-1}$	$\Delta V_{el}^{\ddagger}/cm^3 mol^{-1}$
$[Co^{III}(TNPc^{-2-})]^{2+}/+$	DMF	0.79	-19.9 ± 0.2	1.50 ± 0.01	10.8 ± 0.7	4.1 ± 0.2	11.1 ± 1.0
$[Co^{III/II}(TNPc^{2-})]^{+0}$	DMF	0.38 ^b	-8.6 ± 1.6^b	1.50 ± 0.01	10.6 ± 0.6	0.41 ± 0.02	15.2 ± 0.9
$[Co^{II/I}(TNPc^{2-})]^{0/-}$	DMF	-0.45	-15.5 ± 1.4	2.5 ± 0.1	10.4 ± 0.5	4.7 ± 0.3	21.7 ± 0.2
$[Co^I(TNPc^{2-/3-})]^{-2-}$	DMF	-1.59	-31.6 ± 0.2	3.2 ± 0.1	10.9 ± 0.4	4.6 ± 0.2	12.4 ± 0.9
$[Co^{III}(TNPc^{-2-})]^{2+}/+$	DMA	0.80 ^b	-20.9 ± 1.8^b	1.34 ± 0.04^b	13.4 ± 0.9^b	3.2 ± 0.1	15.6 ± 1.7
$[Co^{III/II}(TNPc^{2-})]^{+0}$	DMA	0.39 ^b	-10.6 ± 1.7^b	1.33 ± 0.02^b	13.9 ± 0.5^b	0.42 ± 0.01	16.7 ± 0.8
$[Co^{II/I}(TNPc^{2-})]^{0/-}$	DMA	-0.43	-14.2 ± 0.7	1.32 ± 0.07	14.9 ± 1.3	2.4 ± 0.2	24.6 ± 1.0
$[Co^I(TNPc^{2-/3-})]^{-2-}$	DMA	-1.61	-29.3 ± 0.8	2.5 ± 0.1	13.3 ± 0.8	5.9 ± 0.1	14.0 ± 0.2
$[Co^{III}(TNPc^{-2-})]^{2+}/+$	DMSO	0.80	-18.8 ± 2.0^c	$1.45 \pm 0.04^{b,c}$	$15.8 \pm 0.8^{b,c}$	3.6 ± 0.1^c	13.4 ± 0.6^c
$[Co^{III/II}(TNPc^{2-})]^{+0}$	DMSO	0.28	-15.7 ± 0.9^c	$1.50 \pm 0.03^{b,c}$	$16.0 \pm 0.5^{b,c}$	0.41 ± 0.01^c	15.0 ± 0.7^c
$[Co^{II/I}(TNPc^{2-})]^{0/-}$	DMSO	-0.51	-21.4 ± 1.2^c	1.42 ± 0.01^c	15.4 ± 0.5^c	3.0 ± 0.1^c	33.9 ± 1.0^c
$[Co^I(TNPc^{2-/3-})]^{-2-}$	DMSO	-1.58	-36.4 ± 3.2^c	2.6 ± 0.1^c	15.1 ± 0.4^c	3.1 ± 0.1^c	13.5 ± 0.3^c
$[Co^{III/II}(TNPc^{-})]^{2+}/+$	DCB	1.04	-16.5 ± 1.2	0.51 ± 0.11	21.8 ± 0.7		
$[Co^{II}(TNPc^{-2-})]^{+0}$	DCB	0.53 ^b	-8.6 ± 1.4^b	2.6 ± 0.1	17.5 ± 0.6		
$[Co^{II/I}(TNPc^{2-})]^{0/-}$	DCB	-0.43 ^b	-10.8 ± 0.6^b	4.9 ± 0.2	18.0 ± 0.9		
$[Co^I(TNPc^{2-/3-})]^{-2-}$	DCB	-1.56	-26.9 ± 2.1	5.0 ± 0.1	16.6 ± 0.2		
$[Co^{III/II}(Pc^{2-})]^{+0}$	Py	0.19	-12.1 ± 2.7	5.1 ± 0.1	11.8 ± 0.4	0.46 ± 0.02	10.8 ± 1.1
$[Co^{II/I}(Pc^{2-})]^{0/-}$	Py	-0.60	-21.7 ± 1.9	5.5 ± 0.1	12.0 ± 0.4		
$[Co^I(Pc^{2-/3-})]^{-2-}$	Py	-1.42	-34.7 ± 0.8	4.8 ± 0.1	11.7 ± 0.5	7.8 ± 0.5	12.5 ± 1.2
$[Fe^{III/II}(Pc^{2-})]^{+0}$	Py	0.67	-29.3 ± 1.4	5.5 ± 0.1	11.2 ± 0.6	9.9 ± 0.3	10.4 ± 0.7
$[Fe^{II/I}(Pc^{2-})]^{0/-}$	Py	-1.10	-27.1 ± 1.6	4.6 ± 0.1	10.8 ± 0.3	9.1 ± 0.8	10.6 ± 1.1
$[Fe^I(Pc^{2-/3-})]^{-2-}$	Py	-1.36	-32.9 ± 1.8	4.7 ± 0.1	10.8 ± 0.6		

^a At Pt wire; 0.3 mol L⁻¹ TBAP; [metallophthalocyanine] = 0.2–0.4 mmol L⁻¹; 25.0 °C except as noted; reference electrode for ΔV_{cell} is Ag/(0.01 mol L⁻¹ AgClO₄ + 0.2 mol L⁻¹ TBAP in CH₃CN). Formulas and net charges given are exclusive of any coordinated anion(s) and solvent. ^b By DPP. ^c 45.0 °C.

Scheme 1. Redox Equations Proposed by Nevin et Al.¹⁹ for CoTNPc in Perchlorate Media (Solvent DMF)



in DMF/0.2 mol L⁻¹ TBAP, the four redox features (right to left) have been attributed^{13,19} to the couples **1–4** in Scheme 1.

The other redox features in Figure 1 have been assigned by comparison with published data.¹³ No features characteristic of adsorption of the electroactive species (known from our companion studies using HOPG electrodes) are evident. The observed peak potentials agree well with those in the literature.¹³ The peak currents for the couples **1–4** were in the ratios 1.0:1.0:1.1:1.5, and the anodic/cathodic current

ratios were 1.0 ± 0.1 . In DPP, the Co^{III}TNPc/Co^{II}TNPc couple **2** gave about half the current of the others, probably because this metal-redox step is too slow (see below) to follow the pulse frequency. For measurements of E_{cell} , D , ΔV_{cell} , and $\Delta V_{diff}^{\ddagger}$, one or at most two couples were scanned at a time; the couples **1** and **2** and the Zn(Pc⁻²⁻) couples were scanned as oxidations, and the others as reductions, but all data in Tables 1 and 2 are reported and discussed in the conventional way as reductions. For ACV measurements of k_{el} and ΔV_{el}^{\ddagger} , each couple was scanned individually.

Values of E_{SCE} (Tables 1 and 2) are on average 0.32 ± 0.08 V more positive than E_{cell} relative to Ag/Ag⁺ and are in good agreement with published data where these exist.^{13,19–23} E_{SCE} values have not been reported previously for the four redox steps of CoTNPc in DMSO and DMA, but those given in Table 2 are close to values reported for these couples in DMF.^{13,19}

For the variable-pressure experiments, potentials (E_{cell}) were referred to Ag/Ag⁺, and only those cycles in which a

(19) Nevin, W. A.; Hempstead, M. R.; Liu, W.; Leznoff, C. C.; Lever, A. B. P. *Inorg. Chem.* **1987**, *26*, 570.

(20) Nyokong, T.; Gasyna, Z.; Stillman, M. J. *Inorg. Chem.* **1987**, *26*, 548.

(21) Lever, A. B. P.; Wilshire, J. P. *Can. J. Chem.* **1976**, *54*, 2514.

(22) Clack, D. W.; Hush, N. S.; Woolsey, I. S. *Inorg. Chim. Acta* **1976**, *19*, 129.

(23) Bernstein, P. A.; Lever, A. B. P. *Inorg. Chem.* **1990**, *29*, 608.

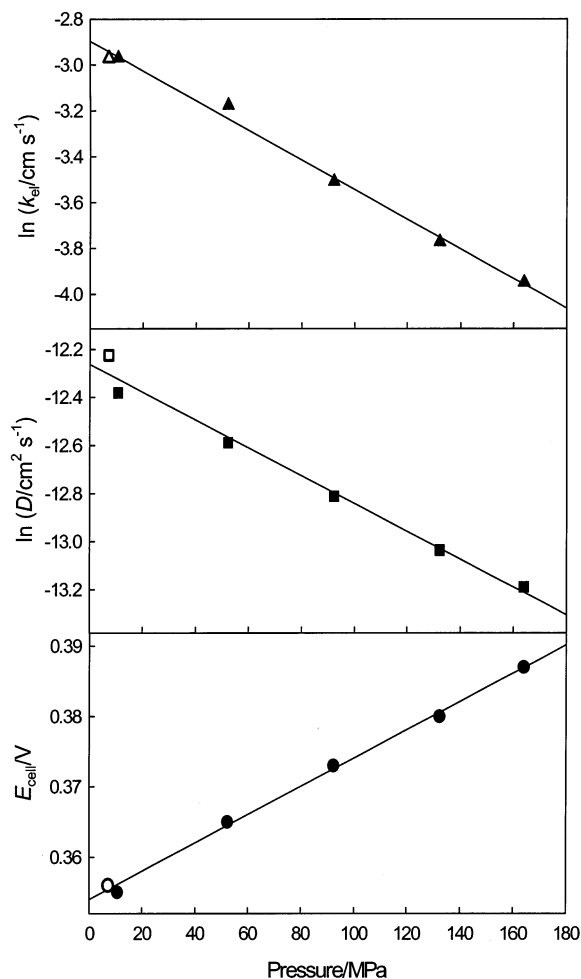


Figure 2. Pressure dependences of E_{cell} relative to Ag/Ag^+ (circles), $\ln D$ (squares), and $\ln k_{\text{el}}$ (triangles) for $[\text{Co}^{\text{III}}(\text{TNPc}^{-2-})]^{2+}/^{+}$ in DMSO at 45.0 °C. Hollow symbols represent measurements made at the end of the pressure cycle.

final low-pressure measurement agreed within the experimental uncertainty with an initial one were accepted. A typical set of acceptable measurements of E_{cell} , $\ln D$, and $\ln k_{\text{el}}$ at variable pressure is shown in Figure 2. In all cases, E_{cell} , $\ln D$ and $\ln k_{\text{el}}$ were linear functions of the applied pressure P within experimental uncertainty (eqs 1, 4, and 5), as is usually found.^{3,4,10,15–18} Thus, for practical purposes, ΔV_{cell} , $\Delta V_{\text{diff}}^{\ddagger}$, and $\Delta V_{\text{el}}^{\ddagger}$ can be taken to be constant over the experimental pressure range of about 0–200 MPa despite theoretical expectations that their numerical values should decrease somewhat with rising pressure.¹⁸ At least, the values of these volume parameters listed in Tables 1 and 2 may be regarded as averages valid at ~ 100 MPa. The values of D and k_{el} given in Tables 1 and 2 were obtained by linear extrapolation of the pressure plots to zero applied (i.e., atmospheric) pressure. The data of Tables 1 and 2 are from representative pressure cycles that met acceptability criteria, and error limits cited are standard deviations representing goodness of linear fit. In general, reproducibility between independent experiments was better than $\pm 2 \text{ cm}^3 \text{ mol}^{-1}$ for ΔV_{cell} , $\Delta V_{\text{diff}}^{\ddagger}$, and $\Delta V_{\text{el}}^{\ddagger}$, $\pm 5 \text{ mV}$ for E_{cell} , and $\pm 10\%$ for D . For the reasons noted above, reproducibility of k_{el} was often poorer than the stated limits suggest, in some cases reaching a factor of about 2, but the k_{el} values tabulated are useful

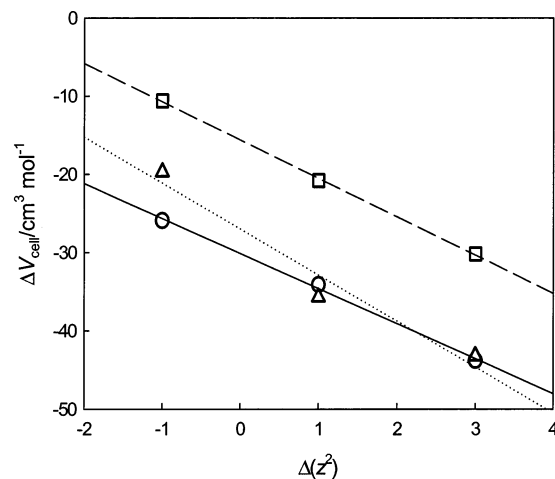


Figure 3. Variation of reaction volumes for ZnPc couples (relative to Ag/Ag^+) with the square of the change in overall charge number of the complex. Solvents are Py at 25.0 °C (circles), DMSO at 45.0 °C (triangles), and DMF at 25.0 °C (squares).

gross measures of the relative rates of the electrode reaction for the various couples considered here. Extensive literature searches retrieved no values of D and k_{el} for appropriate combinations of metallophthalocyanines, solvents, electrodes, and temperature with which our data might be compared.

For certain redox steps (ring oxidation of $\text{Co}^{\text{III}}\text{Pc}^+$ and $\text{Fe}^{\text{III}}\text{Pc}^+$ in Py, first and second ring reductions of ZnPc in DMA), no reliable values could be obtained for D , k_{el} , ΔV_{cell} , $\Delta V_{\text{diff}}^{\ddagger}$, or $\Delta V_{\text{el}}^{\ddagger}$. Reliable values of k_{el} and $\Delta V_{\text{el}}^{\ddagger}$ could not be obtained for any redox step involving CoTNPc in DCB, for the ring oxidation of ZnPc in Py, or for the reductions $\text{Co}^{\text{II}}\text{Pc} \rightarrow \text{Co}^{\text{I}}\text{Pc}$ and $\text{Fe}^{\text{I}}(\text{Pc}^{2-}) \rightarrow \text{Fe}^{\text{I}}(\text{Pc}^{3-})$ in Py.

Discussion

Detailed interpretations of the E_{SCE} data have been given elsewhere^{13,19–23} and need not be repeated here.

Zinc Phthalocyanine. ZnPc provides a reference system in which only the Pc ring is oxidized or reduced.

(a) Volumes of Reaction for ZnPc. Figure 3 shows that, for ZnPc in the solvents Py, DMF, and DMSO, ΔV_{cell} is indeed a linear function of $\Delta(z^2)$ with negative slope, as predicted by eq 3 and demonstrated for aqueous solutions by Tregloan et al.^{2,3} The magnitude of the slope, however, is impossible to predict because the shape of the ZnPc molecule is far from the spherical one that is implicit in eq 3; for example, van der Waals distances from Ni in the analogous compound NiPc range from roughly 0.5 to 1.5 nm in the plane of the Pc ring and 0.17 nm perpendicular to it.²⁴ For the solvents Py and DMF at 25 °C and DMSO at 45 °C, respectively, the slopes in Figure 3 (-4.8 , -4.9 , and $-5.9 \text{ cm}^3 \text{ mol}^{-1}$) and values of Φ (6.6×10^{-11} , 1.82×10^{-11} , and $1.29 \times 10^{-11} \text{ Pa}^{-1}$)^{4,25} correspond to values of the effective radius r of a hypothetical quasi-spherical ZnPc molecule of 1.02, 0.26, and 0.15 nm. These apparent radii might be rationalized qualitatively if we assume that Born-type (continuous dielectric) solvation applies only in direc-

(24) Robertson, J. M.; Woodward, I. *J. Chem. Soc.* **1937**, 219.

(25) Marcus, Y.; Hefter, G. *J. Solution Chem.* **1999**, 28, 575.

tions above and below the Zn center and that ZnPc forms six-coordinate Py_2ZnPc in the powerful donor solvent Py but that the Zn center remains four-coordinate in DMF and DMSO. This interpretation, however, is highly speculative. As ΔV_{cell} was shown⁴ to be linearly dependent on Φ for the decamethylferrocene(+/0) couple (for which $\Delta(z^2)$ is constant at -1), it may be concluded that the problem in accounting for the electrostrictive volume of ions resides in the fictitious nature of r , as has been noted previously even for ions that approximate more closely to spheres.^{2-4,26-28} The essential point is that a linear dependence of ΔV_{cell} on $\Delta(z^2)$ for a given electroactive molecule in a particular solvent is an indication that the molecule does not significantly change its shape or dimensions (including gain or loss of coordinated solvent molecules or counterions) through the successive reductions or oxidations.

(b) Dynamics of the ZnPc Electrode Reaction. With the possible exception of the $\text{Zn}^{\text{II}}(\text{Pc}^{-2-})$ couple in Py (for which dynamic data in general may be unreliable inasmuch as satisfactory k_{el} values could not be obtained), the diffusion coefficients D and especially the corresponding volumes of activation for diffusion $\Delta V_{\text{diff}}^\ddagger$ for ZnPc in a given solvent (Table 1) are similar from one couple to another. Again, this implies that the shape and size of the ZnPc molecule do not change significantly following oxidation or reduction.

Values of the electrode reaction rate constants k_{el} are somewhat scattered, as expected because of the sensitivity to the nature of the electrode surface noted above, but the volumes of activation $\Delta V_{\text{el}}^\ddagger$ are remarkably constant for a given solvent and are close to the corresponding $\Delta V_{\text{diff}}^\ddagger$ values (no kinetic data could be obtained for the possibly anomalous $\text{Zn}^{\text{II}}(\text{Pc}^{-2-})$ case). According to a simple adaptation¹⁸ of Marcus theory of outer-sphere electron-transfer kinetics,²⁹ $\Delta V_{\text{el}}^\ddagger$ for a simple outer-sphere electrode reaction in almost any solvent should be moderately *negative* if transition state theory (TST) is applicable. In fact, all $\Delta V_{\text{el}}^\ddagger$ values in Table 1 are quite strongly *positive*, and their closeness to $\Delta V_{\text{diff}}^\ddagger$ implies that they are similar in magnitude to the volume of activation for viscous flow ($\Delta V_{\text{visc}}^\ddagger$) in the respective solvents. As discussed in detail elsewhere,^{4,15-18} the implication is that if electrode surface effects can be held constant, as they are in a particular variable-pressure experiment, k_{el} would be proportional to the fluidity η^{-1} of the solvent (η is the viscosity of the solvent) as experienced by the electroactive solute. This relationship can arise if TST breaks down because the electrode reaction rate is controlled either by diffusion or by solvent dynamics.^{6,7} In the simplest (Kramers) picture, solvent dynamical rate control occurs when the coupling to solvent motion that propels the reactant(s) up and over the activation barrier (free energy of activation $\Delta G_{\text{el}}^\ddagger$) is strong enough that passage through the transition state is actually hindered. In that case, the preexponential factor Z_{el} in eq 6

$$k_{\text{el}} = Z_{\text{el}} \exp(-\Delta G_{\text{el}}^\ddagger/RT) \quad (6)$$

becomes proportional to the reciprocal of the longitudinal relaxation time τ_L of the solvent, and for practical purposes τ_L is in turn proportional to η in non-hydrogen-bonded solvents,³⁰ whence we expect $\Delta V_{\text{el}}^\ddagger \approx \Delta V_{\text{visc}}^\ddagger \approx \Delta V_{\text{diff}}^\ddagger$ if the contribution of the activation barrier can be neglected. In a more sophisticated approach (see, e.g., Sumi³¹) in which the reaction coordinate and solvent motion coordinate are separated, k_{el} is predicted to be proportional to $\tau_L^{-\alpha}$, where $0 < \alpha < 1$ and $\Delta G_{\text{el}}^\ddagger$ is reduced, whence $\Delta V_{\text{el}}^\ddagger$ should be less than $\Delta V_{\text{diff}}^\ddagger$. Within the accuracy of the present variable-pressure experiments and those reported elsewhere,^{4,15-17} however, it is evident that $\Delta V_{\text{el}}^\ddagger \approx \Delta V_{\text{diff}}^\ddagger$ for electrode reactions of metal complexes in nonaqueous media, and so the simple Kramers-type model is adequate. Evidence gathered to date favors rate control by solvent dynamics rather than diffusion, since at least some of the reactions studied are known to be far from the diffusion-controlled limit^{3,4,6,7,15-18,32-34} (see also the discussion of $\Delta V_{\text{el}}^\ddagger$ for CoTNPC, below). For *aqueous* systems,^{3,10,15,18} the pressure dependence (to ~ 200 MPa) of η at near-ambient temperatures is fortuitously almost nil, and in such cases, $\Delta V_{\text{el}}^\ddagger$ is found to be negative unless anomalies such as counterion-catalyzed pathways dominate. Even for aqueous solutions, however, tuning of the solution viscosity with inert additives reveals a dependence of k_{el} on η^{-1} that implies solvent dynamical effects.^{34,35} It may be concluded that the rates of the various electrode reactions of ZnPc listed in Table 1 are controlled by solvent dynamics.

Cobalt Tetraneopentoxophthalocyanine. The basic question to be addressed here is whether the speciation proposed on the basis of spectroelectrochemical data by Nevin et al.¹⁹ for CoTNPC in DMF (Scheme 1) and in DCB can account for the pressure effects summarized in Table 2. For clarity, the information in Table 2 and Figure 4 is presented without regard for the possibility, raised by Nevin et al.,¹⁹ that ClO_4^- from the supporting electrolyte may be coordinated to $\text{Co}^{\text{III}}\text{TNPC}$ species as in Scheme 1, so changing z . Except in the case of the poor donor solvent DCB, which we discuss separately, a solvent molecule may also be coordinated to the Co center.

(a) Volumes of Reaction for CoTNPC in Donor Solvents. In Figure 4, ΔV_{cell} for CoTNPC in DMF, DMA, and DMSO is plotted against nominal $\Delta(z^2)$ values (i.e., ignoring for the moment the possibility that coordination of ClO_4^- may diminish z). The contrast with the negatively sloping linear dependence of ΔV_{cell} on $\Delta(z^2)$ for ZnPc (Figure 3), in which only ring reductions occur, is striking, implying reduction of the Co^{III} rather than the ring in the second ($\Delta(z^2) = -1$) reduction step, with a corresponding *increase*

- (26) Tran, D.; Hunt, J. P.; Wherland, S. *Inorg. Chem.* **1992**, *31*, 2460.
 (27) Matsumoto, M.; Neuman, N. I.; Swaddle, T. W. *Inorg. Chem.* **2004**, *43*, 1153.
 (28) Bajaj, H. C.; Tregloan, P. A.; van Eldik, R. *Inorg. Chem.* **2004**, *43*, 1429.
 (29) Marcus, R. A.; Sutin, N. *Biochim. Biophys. Acta* **1985**, *811*, 265.

- (30) Zusman, L. D. *Chem. Phys.* **1987**, *112*, 53.
 (31) Sumi, H. In *Electron Transfer in Chemistry*; Balzani, V., Ed.; Wiley-VCH: New York, 2001; Vol. 1, Chapter 2.
 (32) Pyati, R.; Murray, R. W. *J. Am. Chem. Soc.* **1996**, *118*, 1743.
 (33) Williams, M. E.; Crooker, J. C.; Pyati, R.; Lyons, L. J.; Murray, R. W. *J. Am. Chem. Soc.* **1997**, *119*, 10249.
 (34) Zhang, X.; Leddy, J.; Bard, A. J. *J. Am. Chem. Soc.* **1985**, *107*, 3719.
 (35) Zhang, X.; Yang, H.; Bard, A. J. *J. Am. Chem. Soc.* **1987**, *109*, 1916.

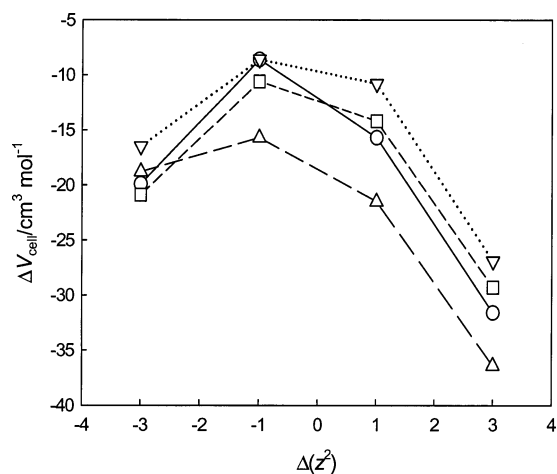


Figure 4. Variation of reaction volumes for CoTNPc couples (relative to Ag/Ag^+) with the square of the change in overall charge number of the complex. Solvents are DMF (circles) at 25.0 °C, DMA at 25.0 °C (squares), DMSO at 45.0 °C (triangles), and DCB at 25.0 °C (inverted triangles).

in volume of the system over and above the expected Drude–Nernst electrostrictive volume decrease such as is seen with ZnPc. This is fully consistent with the assignments made by Nevin et al. for CoTNPc in DMF¹⁹ (and hence by extension for DMA and DMSO also), according to which the second reduction may be identified as $\text{Co}^{\text{III}} \rightarrow \text{Co}^{\text{II}}$ (step 2 in Scheme 1) and the increase in ΔV_{cell} from step 1 to step 2 may be attributed in large part to loss of the coordinated perchlorate ligand. The expulsion of coordinated ClO_4^- from $[\text{Co}^{\text{III}}(\text{solvent})(\text{ClO}_4^-)(\text{TNPc}^{2-})]^0$ following one-electron reduction of the Co^{III} center can be attributed to two factors: first, the introduction of an electron into the antibonding $3d_{z^2}$ orbital with consequent destabilization of the Co–perchlorate bond; second, the formation of a putative *anionic* intermediate $[\text{Co}^{\text{II}}(\text{solvent})(\text{ClO}_4^-)(\text{TNPc}^{2-})]^-$ from which the weakly coordinating anion ClO_4^- would be promptly lost because of electrostatic repulsion. Since ClO_4^- is typically poorly solvated in organic solvents, its expulsion will cause an increase in the volume of the system.

If this scenario is correct, then $\Delta(z^2)$ is actually -1 rather than -3 for the ring-reduction step 1 in Scheme 1, and the change in $\Delta(z^2)$ between this and the other ring-reduction (step 4) is then $+4$. On this basis, by analogy with Figure 3, hypothetical ring-reduction ΔV_{cell} values of about -26 , -26 , and $-28 \text{ cm}^3 \text{ mol}^{-1}$ can be interpolated for the third reduction step in DMF, DMA, and DMSO, respectively, so that the actual values exceed naive expectations by about 10, 11, and (at 45 °C) $6 \text{ cm}^3 \text{ mol}^{-1}$, respectively. Again, these data are consistent with reduction of Co rather than the ring, accompanied by expulsion of a second ligand–coordinated solvent, according to Scheme 1—from the five-coordinate Co^{II} species on reduction to Co^{I} because of the further increase in antibonding $3d_{z^2}$ electron density. Thus, Scheme 1, originally put forward for CoTNPc in DMF,¹⁹ is also applicable to CoTNPc in DMA and DMSO and accounts for the observed values of ΔV_{cell} in these solvents.

(b) Volumes of Reaction for CoTNPc in a Poor Donor Solvent. DCB has no significant tendency to coordinate to metal centers and consequently cannot stabilize Co^{III} relative

to Co^{II} , so the $\text{Co}^{\text{III/II}}$ couple shifts to a potential more positive than ring oxidation.¹³ For the same reason, this potential is very sensitive to anions that can coordinate to Co.¹⁹ Thus, given the predilection of Co^{III} for six-coordination, it is likely that two perchlorates are bound to Co in DCB (cf. the role played by the donor solvent together with ClO_4^- in the $\text{Co}^{\text{III/II}}\text{TNPc}$ redox step in Scheme 1), and the first step on the left for DCB in Figure 4 may be assigned to $[(\text{ClO}_4^-)_2\text{Co}^{\text{III}}(\text{TNPc}^-)] + e^- \rightarrow [(\text{ClO}_4^-)\text{Co}^{\text{II}}(\text{TNPc}^-)] + \text{ClO}_4^-$. The expansion associated with the addition of a $3d_{z^2}$ electron to Co and the concomitant release of a bound perchlorate would explain why ΔV_{cell} for the first step in DCB is not very different from that for the first step in DMF, DMA, and DMSO, despite the much more negative Drude–Nernst contribution ΔV_{solv} expected for DCB (eq 3; $\Phi = 9.7 \times 10^{-11} \text{ Pa}^{-1}$ for DCB, cf. $1.8 \times 10^{-11} \text{ Pa}^{-1}$ for DMF^{4,25,36}). The second step in DCB is then attributable to ring reduction in $\text{Co}^{\text{II}}(\text{TNPc}^-)$, which might be expected (cf. ZnPc) to give a markedly more *negative* ΔV_{cell} than the first step; in fact, the second step gives ΔV_{cell} $8 \text{ cm}^3 \text{ mol}^{-1}$ more *positive* than the first, consistent with loss of the second bound perchlorate.

The third reduction step in DCB differs from those in DMF, DMA, and DMSO in that there is no coordinated solvent to be lost (Scheme 1), and Φ and presumably r are quite different, so that interpretation of the relative ΔV_{cell} values is not presently feasible. Taking all the ΔV_{cell} data for CoTNPc and ZnPc together, one can say, regardless of detailed interpretation, that whereas consecutive ring reductions result in progressive increases in electrostriction of solvent according to eq 3 (Figure 3), reductions of the metal center in CoTNPc result in much less negative values of ΔV_{cell} than would be expected by analogy with ring reductions of the same charge type.

(c) Diffusion Coefficients for CoTNPc. Most of the mean diffusion coefficients D for CoTNPc couples (Table 2) are of similar magnitude in DMF and DMA, which have about the same viscosity ($\eta = 0.8\text{--}0.9 \text{ mPa s}$ at 25 °C; the DMSO data are for 45 °C, at which $\eta \approx 1.3 \text{ mPa s}$).³⁶ In the donor solvents DMF, DMA, and DMSO, D is effectively constant over successive reductions except for a modest rise on going to the fourth couple, in which no coordinated anion or solvent is thought to be present (Scheme 1) and for which the hydrodynamic bulk of the complex should be correspondingly smaller. The implication is, once again, that the sizes of the electroactive species are not greatly changed in successive redox processes unless axial ligands are lost.

The conspicuously low D for the $[\text{Co}^{\text{III}}(\text{TNPc}^-)]^{2+}/[\text{Co}^{\text{II}}(\text{TNPc}^-)]^+$ couple in DCB is attributable to the somewhat higher viscosity of this solvent (1.3 mPa s)³⁶ relative to DMF and DMA, together with a large hydrodynamic bulk due to the inferred axial coordination of two perchlorates to each of these cations in this poorly complexing solvent of low dielectric constant. An alternative possibility is that the complexes are aggregated, as reported for CoPc in DMSO,³⁷

(36) *Organic Solvents: Physical Properties and Methods of Purification*, 4th ed.; Riddick, J. A., Bunger, W. B., Sakano, T. K., Eds.; Wiley-Interscience: New York, 1986.

(37) Owlia, A.; Rusling, J. F. *J. Electroanal. Chem.* **1987**, *234*, 297.

although this phenomenon may simply reflect the poor solubility of CoPc in DMSO²² and, besides, the bulk of the TNPC ligand would work against aggregation. For the third and fourth couples, the higher viscosity of DCB relative to DMA and DMF is evidently compensated by reduced hydrodynamic bulk of CoTNPC due to the lack of axial ligands. For the second couple ($[\text{Co}^{\text{II}}(\text{TNPC}^-)]^+ / [\text{Co}^{\text{II}}(\text{TNPC}^{2-})]$), D in DCB is half that of the third and fourth couples, consistent with the foregoing suggestion that one coordinated perchlorate remains.

The volume of activation for diffusion $\Delta V_{\text{diff}}^\ddagger$, which represents a property of the solvent ($\Delta V_{\text{visc}}^\ddagger$) rather than of the redox-active solute, is effectively constant from one redox step to another within a given solvent, but increases in the sequence DMF < DMA < DMSO < DCB.

(d) Kinetics of the CoTNPC Electrode Reaction. The most striking feature of the electrode reaction rate constants k_{el} for the four CoTNPC couples in DMF, DMA, and DMSO is that the second reduction reaction (assigned to $\text{Co}^{\text{III}} \rightarrow \text{Co}^{\text{II}}$) is about 10 times slower than the others, for which k_{el} values are about the same in a given solvent (with allowance for the difficulty noted above in obtaining definitive k_{el} values). This observation rules out diffusion control of the electrode reaction rates, since D is effectively the same for the first, second, and third couples. The slowness of the $\text{Co}^{\text{III}} \rightarrow \text{Co}^{\text{II}}$ step is as expected on the basis of Marcus theory²⁸ because the addition of an antibonding $3d_{z^2}$ electron to Co^{III} in the six-coordinate $[(\text{solvent})(\text{ClO}_4)_4\text{Co}^{\text{III}}\text{TNPC}]^0$ complex should produce major structural distortions and Franck–Condon restrictions, leading ultimately to loss of the perchlorato ligand. Thus, k_{el} and $\Delta V_{\text{el}}^\ddagger$ for this step may be composite quantities.

We saw with ZnPc (Table 1) that $\Delta V_{\text{el}}^\ddagger$ was essentially the same for each successive ring reduction in a given solvent and roughly equal to $\Delta V_{\text{diff}}^\ddagger$. Table 2 shows that this is also true for the ring-reduction steps **1** and **4** of CoTNPC. For step **2**, $\Delta V_{\text{el}}^\ddagger$ is only slightly ($2\text{--}3 \text{ cm}^3 \text{ mol}^{-1}$) more positive than for the corresponding ring reductions, which contrasts with the much larger positive deviations in ΔV_{cell} (Figure 4), but for all three steps **1**, **2**, and **4** $\Delta V_{\text{el}}^\ddagger$ is very close to $\Delta V_{\text{diff}}^\ddagger$, indicating a dominant role of solvent dynamics in controlling the electrode reaction rates,^{3,4,15–18} just as with ZnPc. The slowness of step **2** despite the normal corresponding diffusion coefficient, however, affirms that factors that determine the activation barrier height remain important, as in Marcus (TST-based) theory. The smallness of the excess in $\Delta V_{\text{el}}^\ddagger$ for step **2** over those for **1** and **4** (in which the first coordination sphere of Co remains unchanged, according to Scheme 1) suggests that loss of the perchlorato ligand in process **2** may occur rapidly *after* a slow, rate-determining reduction of the substitution-inert Co^{III} center. In contrast, $\Delta V_{\text{el}}^\ddagger$ for the relatively rapid step **3** ($\text{Co}^{\text{II}} \rightarrow \text{Co}^{\text{I}}$) is $10\text{--}20 \text{ cm}^3 \text{ mol}^{-1}$ more positive than for ring reductions, depending on the solvent, and may reflect loss of coordinated solvent from the comparatively labile Co^{II} center *before* the rate-determining step in the electrode reaction is reached. Furthermore, $\Delta V_{\text{el}}^\ddagger$ for step **3** is much larger than $\Delta V_{\text{diff}}^\ddagger$ in all three solvents, implying that factors in addition to solvent

dynamics are involved in the approach to and crossing of the activation barrier for that step and effectively ruling out diffusion control of the electrode reaction rate.

Cobalt Phthalocyanine. The solubilities of CoPc and FePc are poorer than that of ZnPc in most solvents,²² and in any event problems due to aggregation of CoPc and (to a lesser degree) FePc in DMSO³⁷ and presumably other relatively weak donor solvents were anticipated. Our comparative studies of these complexes were therefore limited to the strong donor solvent pyridine, in which the Co^{II} and Co^{III} species are of the type $[\text{Py}_2\text{CoPc}]^{21}$ although, even in Py, we were unable to obtain useful data on Pc ring reduction in $[\text{Py}_2\text{Co}^{\text{III}}(\text{Pc}^-)]^{2+}$ (corresponding to step **1** in Scheme 1). Nevertheless, the CoPc data provide a more appropriate comparison to the ZnPc results than do those of the bulky CoTNPC. Table 2 shows that ΔV_{cell} for the reductions of Co^{III} to low-spin²¹ $[\text{Py}_2\text{Co}^{\text{II}}(\text{Pc}^-)]$ and of Co^{II} to Co^{I} (cf. steps **2** and **3** in Scheme 1) are more positive by 14 and $12 \text{ cm}^3 \text{ mol}^{-1}$, respectively, than for the ZnPc couples of the same charge type in Py (Table 1). As the latter are Pc ring reductions, the positive excesses in ΔV_{cell} for the CoPc couples can be attributed to reductions of the metal center in the same manner as for CoTNPC in other donor solvents in steps **2** and **3** of Scheme 1. The reduction of $\text{Co}^{\text{I}}(\text{Pc}^{2-})$ is evidently a ring reduction,¹³ analogous to step **4** of Scheme 1, and the further decrease in ΔV_{cell} can be attributed to increased Drude–Nernst electrostriction as for ZnPc.

The diffusion constants and $\Delta V_{\text{diff}}^\ddagger$ for CoPc species in Py are effectively the same for all, but the rate constant k_{el} for the $\text{Co}^{\text{III}} \rightarrow \text{Co}^{\text{II}}$ step is $17\text{--}29$ times smaller than k_{el} for the ring reductions of either $\text{Co}^{\text{I}}(\text{Pc}^{2-})$ or any of the ZnPc species in Py (Tables 1 and 2). As discussed above for $\text{Co}^{\text{III/II}}(\text{TNPC}^{2-})$, this is attributable to Franck–Condon restrictions associated with the distortions evident in ΔV_{cell} . Values of $\Delta V_{\text{el}}^\ddagger$ are similar to $\Delta V_{\text{diff}}^\ddagger$ for both the Co^{III} and the ring reductions in Py, as found for the analogous CoTNPC couples in other solvents and consistent with dominant solvent dynamical control of the reaction rates. In general, the behavior of the CoPc couple in Py parallels that for CoTNPC in various solvents, despite evidence¹³ that six-coordination for CoPc in Py is achieved with two Py ligands and for CoTNPC in other donor solvents with one perchlorato and one solvent ligand.

Iron Phthalocyanine. At equilibrium in pyridine, $\text{Fe}^{\text{III}}\text{Pc}$ and $\text{Fe}^{\text{II}}\text{Pc}$ are present as six-coordinate $[\text{Py}_2\text{Fe}^{\text{III}}(\text{Pc}^{2-})]^+$ and $[\text{Py}_2\text{Fe}^{\text{II}}(\text{Pc}^{2-})]$ (low-spin $3d^5$ and $3d^6$) and $\text{Fe}^{\text{I}}\text{Pc}$ as five-coordinate $[\text{PyFe}^{\text{I}}(\text{Pc}^{2-})]^-$ (low-spin $3d^7$), but further reduction of the Fe^{I} complex occurs as ring reduction without loss of the coordinated Py.^{38,39} Since the reduction of $[\text{Py}_2\text{Fe}^{\text{III}}(\text{Pc}^{2-})]^+$ to $[\text{Py}_2\text{Fe}^{\text{II}}(\text{Pc}^{2-})]$ involves addition of an essentially nonbonding electron at Fe, ΔV_{cell} for this step is only a little more negative than that for the ring-reduction of $[\text{Py}_2\text{Zn}(\text{Pc}^-)]^+$, which involves the same $\Delta(z^2)$, but much more negative than for the reduction of $[\text{Py}_2\text{Co}^{\text{III}}(\text{Pc}^{2-})]^+$ to $[\text{Py}_2\text{Co}^{\text{II}}(\text{Pc}^{2-})]$ in which an antibonding electron is intro-

(38) Stillman, M. J.; Thomson, A. J. *J. Chem. Soc., Faraday Trans. 2* **1974**, *70*, 790.

(39) Lever, A. B. P.; Wilshire, J. P. *Inorg. Chem.* **1978**, *17*, 1145.

duced at the Co center (Tables 1 and 2). Reduction of $[\text{Py}_2\text{Fe}^{\text{II}}(\text{Pc}^{2-})]$, however, adds an antibonding $3d_{z^2}$ electron to the Fe center, leading to distortion of the complex and ultimately to loss of one of the Py ligands. Thus, despite the greater $\Delta(z^2)$ for this second reduction, ΔV_{cell} is a little more positive for this step than for the $\text{Fe}^{\text{III/II}}$ reduction and substantially more so than for the $[\text{Py}_2\text{Zn}(\text{Pc}^{2-})]$ ring reduction which has the same $\Delta(z^2)$. For Pc ring reduction in $[\text{PyFe}^{\text{I}}(\text{Pc}^{2-})]^-$, ΔV_{cell} is more negative than for the preceding step, as expected qualitatively from the larger $\Delta(z^2)$, and is close to that for the analogous ring reduction in $[\text{PyCo}^{\text{I}}(\text{Pc}^{2-})]^-$.

Mean diffusion coefficients D for the FePc couples in Table 2 are essentially equal to each other and to those for the corresponding CoPc couples, and the same is true for $\Delta V_{\text{diff}}^\ddagger$. For the $\text{Fe}^{\text{III/II}}$ and $\text{Fe}^{\text{II/I}}$ couples, the rate constants k_{el} are about equal, as are $\Delta V_{\text{el}}^\ddagger$, which, in turn, are close to the corresponding $\Delta V_{\text{diff}}^\ddagger$, implying that solvent dynamics dominate the FePc reaction rates.

Conclusions. As this study was the first to explore the high-pressure electrochemistry of metallophthalocyanines in solution, technical difficulties were encountered that limited the extent of information that could be gleaned. In particular, the poor solubility of CoTNPC in Py, and of CoPc and FePc in all other solvents, precluded a direct comparison of these redox systems. Moreover, some key k_{el} and $\Delta V_{\text{el}}^\ddagger$ values could not be measured accurately. The ZnPc species, however, are sufficiently soluble in several solvents to provide enough common ground to make several deductions. Measurements on ZnPc showed that ΔV_{cell} for successive Pc ring reductions is linearly dependent on $\Delta(z^2)$ (Figure 3), consistent with the Drude–Nernst relation (eq 3), albeit with a fictitious effective radius r because of the wide departure of the Pc complexes from spherical shape. Measurements on CoTNPC, CoPc, and FePc, however, showed that steps involving insertion of one or more antibonding ($3d_{z^2}$) electrons on the metal center have ΔV_{cell} values much more positive than expected from interpolation of ring-reduction data (Figure 4 and Table 2). These positive deviations can

be attributed to distortions of, and particularly axial ligand loss from, the metallophthalocyanines. In general, the ΔV_{cell} data for metal-center reduction are consistent with information from other sources^{13,19,21,38,39} on complexation of the metal by donor solvents and by the anion of the supporting electrolyte.

Although rate constants k_{el} for the electrode reactions tended (as usual) to be somewhat scattered, it was clear that the $\text{Co}^{\text{III}}\text{TNPC}$ and $\text{Co}^{\text{III}}\text{Pc}$ reductions were an order of magnitude slower than the other electrode reactions, for which k_{el} varied only within a narrow range for a particular metallophthalocyanine and solvent. This is as expected for reductions of low-spin $3d^6$ to $3d^7$, for which concomitant structural distortions of the complex (including possible axial ligand dissociation) should retard the reaction via the Franck–Condon factors. The volumes of activation $\Delta V_{\text{el}}^\ddagger$, however, were invariably positive and in most cases roughly equal to $\Delta V_{\text{diff}}^\ddagger$, indicating predominant rate control by solvent dynamics rather than by activation in the manner of TST for which negative $\Delta V_{\text{el}}^\ddagger$ would be expected. The fact that some reactions in a reduction series were anomalously slow shows that $\Delta G_{\text{el}}^\ddagger$ in eq 6 is still important, even if solvent dynamical control through Z_{el} dominates. By the same token, diffusion control of the reaction rates can be ruled out in favor of solvent dynamics.

Work continues in our Calgary laboratory on variable-pressure studies of metallophthalocyanines in aqueous solution and adsorbed on electrodes.

Acknowledgment. We thank Dr. C. C. Leznoff for donation of some phthalocyanine complexes for our exploratory studies and the Natural Sciences and Engineering Research Council of Canada for financial support. A.B.P.L. thanks the Canada Council for the Arts for a Killam Fellowship (2000–2002).

Supporting Information Available: Figure S1, showing the construction of the electrochemical cell. This material is available free of charge via the Internet at <http://pubs.acs.org>.

IC040032D